Clima p 131

PREDICTION OF THERMAL COMFORT IN A ROOM WITH A COLD AIR DIFFUSION SUPPLY UNIT

A. MESLEM [1,2], C. INARD[1], P. BARILES[2]
[1] CETHIL/T13, IINSA 135t 307
20, av. Albert Einstein F69621 VILLEURBANNE

[2]CETIAT 27/29 Bld du 1 1 Novembre 1918
B.P. 6084 F69604 VILLEURBANNE

ABSTRACT

Indoor air flow induced by a fan-coil unit in an air-conditioned environmental chamber is studied experimentally. The supply Archimedes number which is a macroscopic number describing indoor air flow is measured and related to the centreline velocity and temperature decay of the cold air jet issued from the fan-coil unit. The space air diffusion and the thermal comfort using respectively the Air Diffusion Performance Index (ADP]) and the Predicted Percentage of Dissatisfied (PPD) are evaluated. Evolution of these indices with the supply Archimedes number is discussed.

KEYWORDS
Negative buoyant jet, Space air diffusion, Thermal comfort, Air diffusion performance.

1. INTRODUCTION

The purpose of air-conditioned systems is to maintain suitable conditions in an indoor environment. Conditioned air should be supplied in proper quantities and temperatures to reach various thermal requirements of occupied spaces. Large air velocities and temperature gradients should be avoided since these factors, either individually or combined, may cause undesirable conditions for occupants in airconditioned spaces. When these factors are induced by the main driving flows which are respectively the cold air jet issued from the air conditioned system and the plumes created by internal heat loads, it seems important in order to study thermal comfort in the occupied spaces, to well know the behaviour laws of these driving flows and particularly of the cold air jet.
Our experimental work is performed to analyse the fan-coil unit cold air jet and to try to rely it with the indoor thermal comfort and the air diffusion performance.

2. EXPERIMENTAL ARRANGEMENT

Experiments were conducted in the CETIAT air-conditioned test chamber located in Villeurbanne, France. Figure 1 presents the longitudinal section of the experimental set-up, made of a single cell of volume 4.9x2.8x2.8 m^3 bounded on five sides by air volumes regulated at a constant temperature level (+25°C for the present study). The sixth side, called the facade, is submitted to the influence of a climatic housing where we can simulate external air temperature variations. For these experiments, this temperature has been set to the value of +38°C. Furthermore, electric films uniformly distributed over the floor are used in order to simulate internal heat loads. These loads are balanced, that is to say, for an ambient temperature around +25°C, by a hydronic room fan-coil unit (0.97m long and 0.70m high) placed against the facade. The dimensions of the fan-coil unit supply grille are 0.4xO. 06 m2. Concerning the cold air jet, we used a crossed hot fibre film probe, type DANTEC 55R52 running in the constant temperature mode to sense the flow velocity, and a cold wire probe type DANTEC 55P31 running in the constant current mode to sense the flow temperature. Both probes are coupled to a computerized digital data acquisition system. For simultaneous measurements of velocity and temperature in the flow, the temperature probe is placed slightly upstream (5mm) and offset (2mm) from the velocity probe. This separation was chosen as a suitable compromise, since a too small separation yields contamination of the temperature sensor by the thermal wake of the hot fibre films, while a too wide separation would increase the spatial resolution unacceptably [Antonia and Chambers 1980]. To minimise scatter, a low pass filter with a cut-off frequency of 80Hz associated with a long integration time (1 mn) and an acquisition frequency of 200Hz were used.
The velocity probe was calibrated for the desired velocity range and flow direction, according to the Cosines Law method developed by Jorgensen (1971), and using the automatic calibrator for hot-wire anemometers developed by DANTEC [Stannov 19951. The calibration curve of the cold wire probe was obtained with a calibration air chamber. During the measurements, air temperature values were also used to compensate velocity data for temperature change. In order to explore the whole jet, these probes were mounted on an automatic displacement apparatus.
The air velocities and temperatures in the occupied zone of the room were measured with 12 thermoanemometric sensors [Calvet and Liousse 1971] placed at 80 different locations in the occupancy zone of the room. At each position, measurements were taken during a 15 minute period in order to obtain representative mean air velocities and temperatures. These probes have been calibrated using CETIAT velocity and temperature calibration facilities. The inner wall surface temperatures were measured with 10U2 RTD probes calibrated at the laboratory. At last, indoor relative humidity was measured with a capacitive hygrometer.

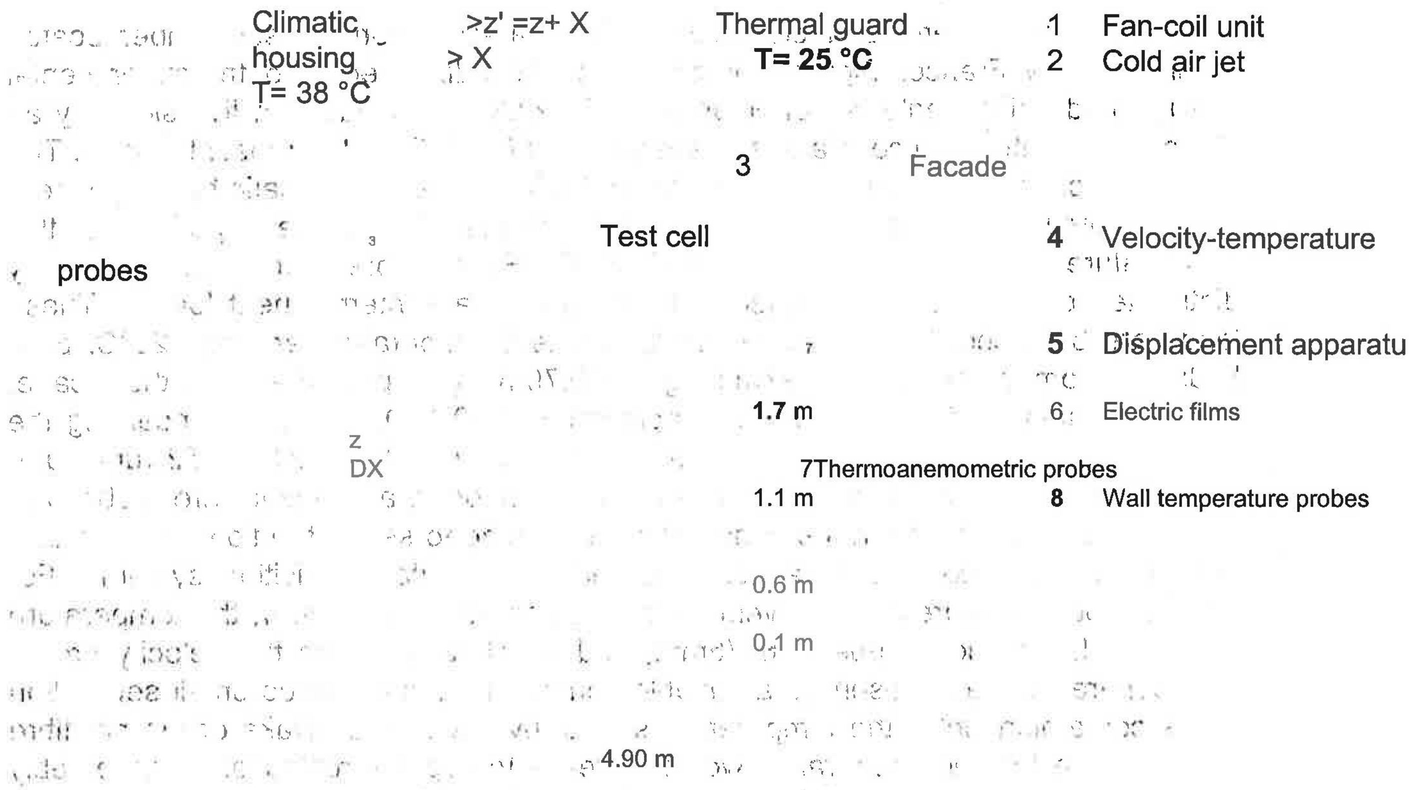

Figure 1. Longitudinal section of the experimental set-up.

3. TEST CONDITIONS

18 tests were carried out under a variety of room loads and air flow rate conditions. The parameters used for the experiments are summarized in table 1. All test data were obtained during conditions of thermal equilibrium.

Test No.	Q0 (M 3 /h)	q (W)	U0 (m/S)	TO (0c)	DTO (OC)	Aro x104
1	285	0	3.16	26.5	0	0
2	291	0	3.24	22.6	3.4	5.0
3	268	0	2.98	22.1	3.9	6.5
4	246	0	2.74	20.4	4.9	10.3
5	278	500	3.10	19.5	6.4	10.4
6	216	0	2.40	21.4	4.3	11.6
7	268	500	2.98	18.6	6.9	12.1
8	281	1150	3.14	14.9	10.1	16.0
9	239	500	2.66	18.2	7.5	16.6
10	284	1100	3.16	14.3	10.7	16.7
11	261	1150	2.92	14.6	10.4	19.1
12	177	0	1.97	19.2	5.9	23.8
13	243	970	2.71	14.1	11.4	24.2
14	204	500	2.27	16.1	8.9	26.9
15	207	900	2.32	14.0	12.2	35.3
16	175	300	1.95	14.2	10.4	42.8
17	167	500	1.86	14.7	11.1	50.2
18	169	700	1.88	13.0	12.8	56.6

Table 1 Experimental conditions.

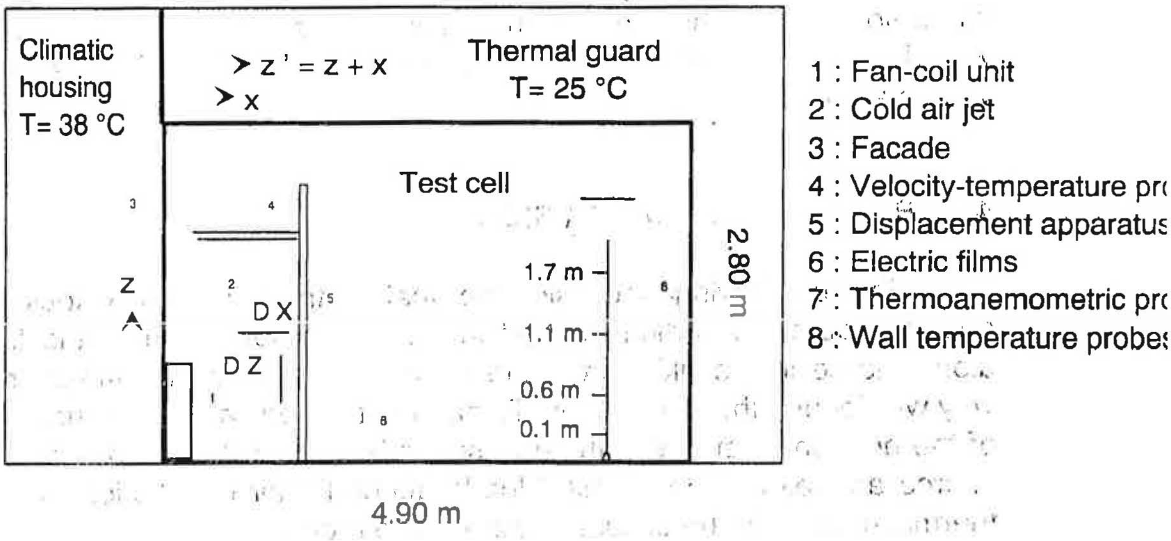

Figure 1. Longitudinal section of the experimental set-up.

3. TEST CONDITIONS

18 tests were carried out under a variety of room loads and air flow conditions. The parameters used for the experiments are summarized in table 1 test data were obtained during conditions of thermal equilibrium.

Test No.	Q_0 (m^3/h)	q (W)	U_0 (m/s)	T_0 (°C)	DT_0 (°C)	$Ar_0 \times 10^4$
1	285	0	3.16	26.5	0	0
2	291	0	3.24	22.6	3.4	5.0
3	268	0	2.98	22.1	3.9	6.5
4	246	0	2.74	20.4	4.9	10.3
5	278	500	3.10	19.5	6.4	10.4
6	216	0	2.40	21.4	4.3	11.6
7	268	500	2.98	18.6	6.9	12.1
8	281	1150	3.14	14.9	10.1	16.0
9	239	500	2.66	18.2	7.5	16.6
10	284	1100	3.16	14.3	10.7	16.7
11	261	1150	2.92	14.6	10.4	19.1
12	177	0	1.97	19.2	5.9	23.8
13	243	970	2.71	14.1	11.4	24.2
14	204	500	2.27	16.1	8.9	26.9
15	207	900	2.32	14.0	12.2	35.3
16	175	300	1.95	14.2	10.4	42.8
17	167	500	1.86	14.7	11.1	50.2
18	169	700	1.88	13.0	12.8	56.6

Table 1 : Experimental conditions.

The Archimedes number $Ar_o = g\beta DT_0h_0/U_0^2$ is used to characterize the supply conditions. In the calculation of Aro, we used the effective width (ho) of the supply grille. Mean values of exit temperature and velocity were obtained by measuring the temperature and velocity profiles over a 8x12 mesh (Dx = 5cm and Dy = 0.5cm). The integration of the velocity profiles over the grille area allows us to calculate the air mass flow rate of the fan-coil unit. The values thus obtained have been compared with those calculated using the water heat balance. The differences between these values are less than 15%.

4. RESULTS AND DISCUSSION

In the following discussion we analyse the centreline velocity and temperature decay in both the vertical wall jet induced by a fan-coil unit and the horizontal flow along the ceiling resulting from the vertical jet bend at the wall/ceiling corner. In this way we deduce the penetration distance of the vertical jet and the separation distance of the horizontal jet. We further describe how the initial conditions of the air diffusion source as well as internal heat loads affect the air distribution performance and the thermal comfort in the occupied zone of the room.

4.1. Cold air jet characteristics

Figure 2 presents the decay of the centreline velocity and temperature for all the tests. From the Figure 2, we can distinguish three types of cold air jet behaviour according to the Archimedes number values. For the Archimedes number values less than 0.00121 (tests 1 to 7), the jet reaches the ceiling and the decay of the centreline velocity and temperature of the jet can be described by relations close to those usually used for linear isothermal wall jets [Rajaratnam, 1976]. Considering higher Archimedes number values (tests 8 to 13), the jet also reaches the ceiling but. along this surface, we can notice the influence of the negative buoyancy which tends to reduce the jet penetration. At last, for tests 14 to 18 which were carried out with the higher Archimedes number values, the vertical cold air jet does not reach the ceiling and a reverse flow occurs resulting in a self feeding of the jet as it appears on the decay of the centreline temperature.

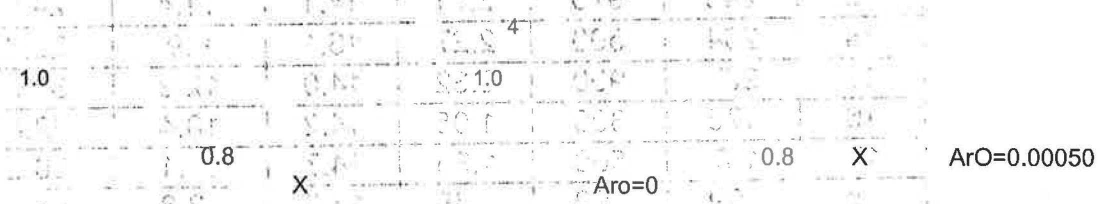

ArO=0.00050

1 : Aro=0.00065

0.6 Aro=0.00065 0.6 X Aro=0.00103

Aro=0.00103 0

@)K A ro=0.001 04 Aro=0.00104

0.4)K Aro=0.00116 0.4 Aro=0.00116

C

Aro=0.00121 x Aro=0.00121

X

0.2 0.2

all

'X@ %@

0.0 0.0

0 2 0 40 6 0 8 0 100 120 140 160 0 20 40 60 80 100 120 140 160

1.0 + Aro=0.00160 1.0 +

Aro=0.00160

0.8 -Aro=0.00166 0.8 Aro=0.00

ArO=0.00167 ArO=0.0

Aro=0.00191 0.6 Aro=0.00

0.6 ArO=0.00238 ArO=0.0

Aro=0.00242 Aro=0.00

0.4

0.4 ebb

P

0.2 rr

0.2

0.0 +

0.0 0 20 40 60 80

0 20 40 60 80 100 -0.2

1.0 Aro=0.00269 1.0

0 Aro=0.00269

0 Aro=0.00353 0 Aro=0.00353

0.8 Aro=0.00428 0.8 Aro=0.00428

Aro=0.00502 Aro=0.00502

0.6 <> Aro=0.00566 0.6 Aro=0.00566

M' 0.4 0.4

0.2 0.2

001

0 00: F1 0

0.0 0 0.0 0 A n

0 10 20 30 40 50 -0.2 z'lh, 0

z'lh, 0 10 20 30 4On so

Figure 2. Decay of the centreline velocity and temperature of the cold air jet.

4.1.1. Vertical jet analysis

We can describe the vertical jet by using a general scaling law as proposed by Grimitlyn and Pozin (1993). So, the decay of the centreline velocity and temperature can be defined by.

)]0-5 3/2 1113 (3)

U,/UO = Kv [hJ(z+zo
DTM/DTO = KT [hJ(z+zo)l C.9 /Kn
K, = [1 - A (KT/K, 2) Aro ((z+zo)/ho)

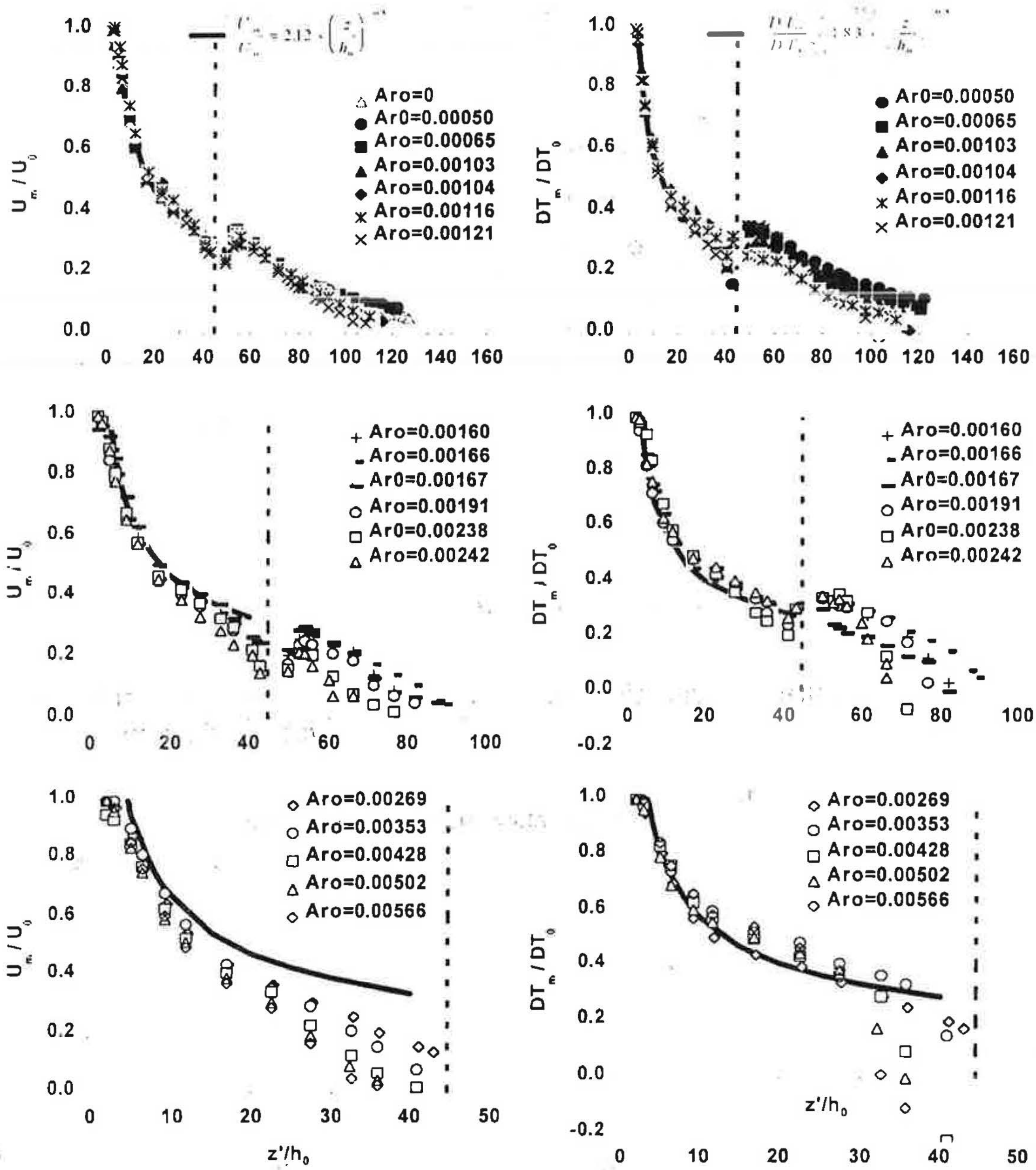

Figure 2. Decay of the centreline velocity and temperature of the cold air jet.

4.1.1. Vertical jet analysis

We can describe the vertical jet by using a general scaling law proposed by Grimitlyn and Pozin (1993). So, the decay of the centreline velocity a temperature can be defined by:

$$U_m/U_0 = K_v\,[h_o/(z+z_0)]^{0.5}\,K_n \tag{1}$$
$$DT_m/DT_0 = K_T\,[h_o/(z+z_0)]^{0.5}\,/K_n \tag{2}$$
$$K_n = [1 - A\,(K_T/K_v^2)\,Ar_0\,((z+z_0)/h_0)^{3/2}\,]^{1/3} \tag{3}$$

The centreline velocity and temperature constants KV and κ_T as well as the virtual or value zo are obtained with tests 1 to 3 for which the negative buoyancy is zero or negligible (Figure 3), On the other hand a A value equal to 2.87 is estimated with tests 4 to 18 (see Fig 4). For linear free jets, the A value is equal to 1.80 [Grimitlyn and Pozin 19931 which is lo than the one found here. We think that it is due, for the wall jet, to a lower ambient entrainment resulting in a larger influence of the exit Archimedes number on the characteristics.

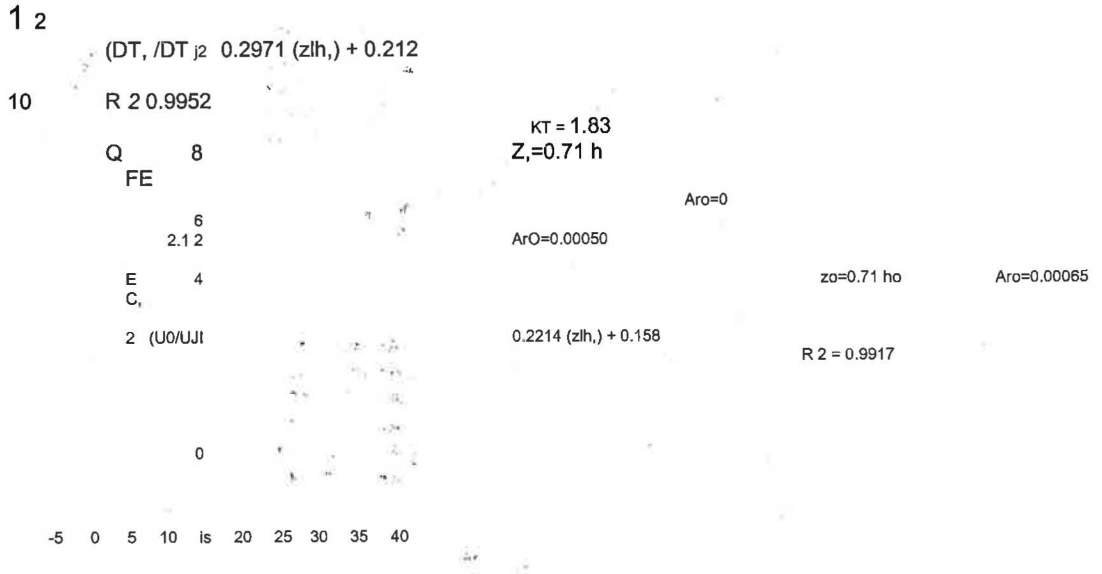

Figure 3. Evaluation of the centreline velocity an temperature constants KV and κ_T and virtual origin zo

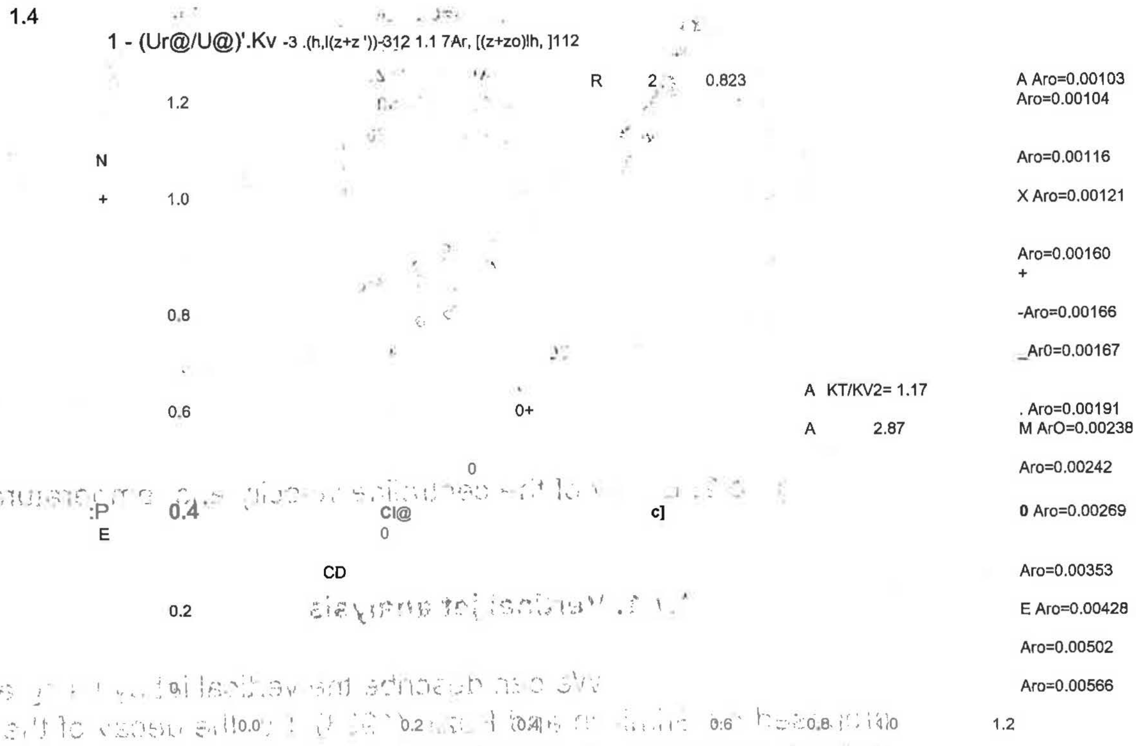

Aro .[(z+zo)lh 0 312

Figure 4. Decay of the centreline velocity of the cold vertical wall jet.

The theoretical value of the jet penetration is defined at the location where the velocity valu zero. Here, it is difficult to get a jet penetration with this criteria because of the confinement eff So, as proposed by Goldman and Jaluria(1986),

The centreline velocity and temperature constants K_v and K_T as well as the vir
origin value z_0 are obtained with tests 1 to 3 for which the negative buoyancy is z
or negligible (see Figure 3). On the other hand a A value equal to 2.87 is estima
with tests 4 to 18 (see Figure 4). For linear free jets, the A value is equal to ´
[Grimitlyn and Pozin 1993] which is lower than the one found here. We think that
due, for the wall jet, to a lower ambient air entrainment resulting in a larger influe
of the exit Archimedes number on the jet characteristics.

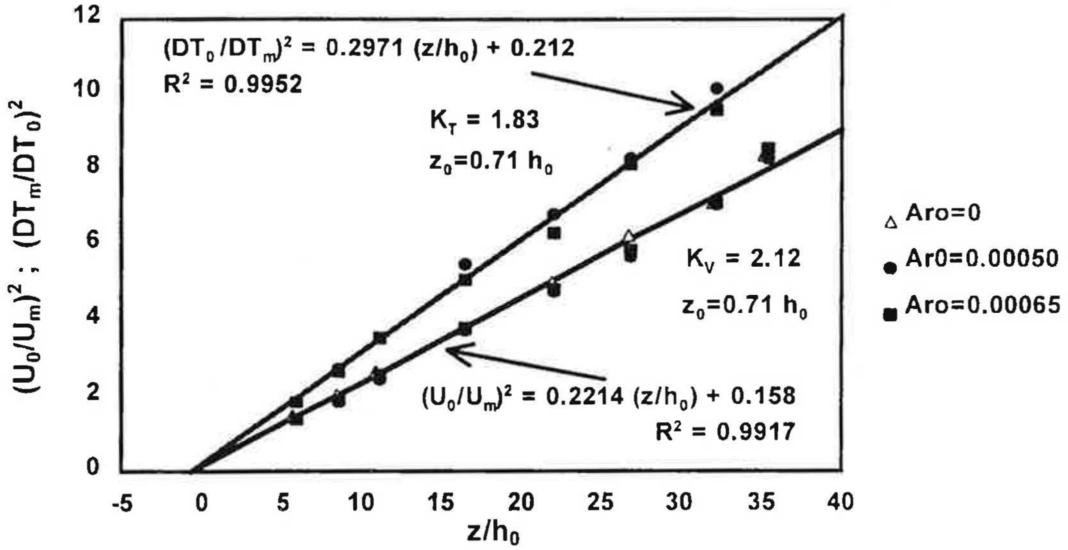

Figure 3. Evaluation of the centreline velocity an temperature constants K_v and K
and the virtual origin z_0

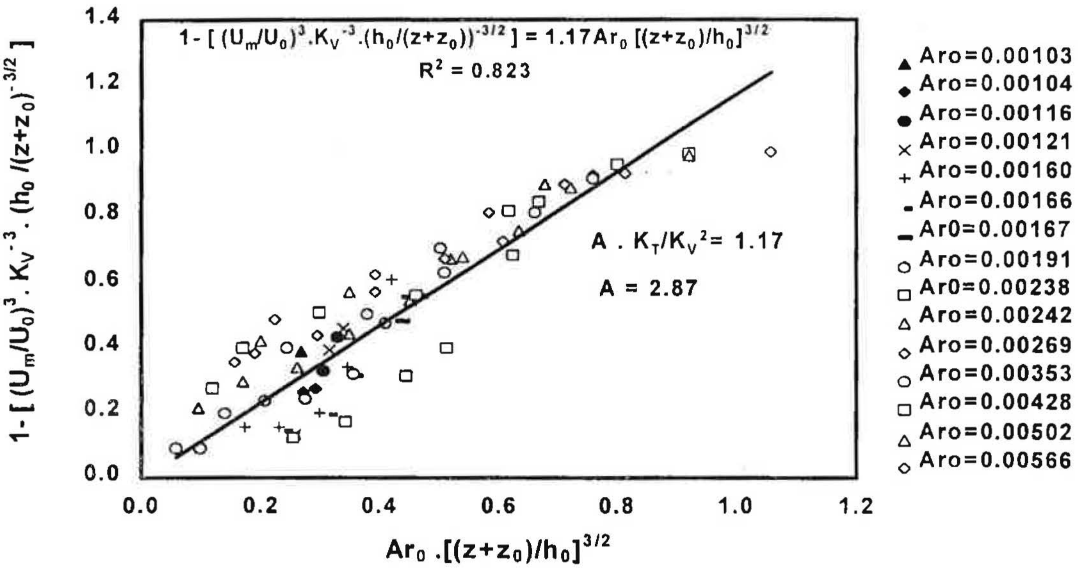

Figure 4. Decay of the centreline velocity of the cold vertical wall jet.

The theoretical value of the jet penetration is defined at the location where t
velocity value is zero. Here, it is difficult to get a jet penetration with this crite
because of the confinement effect. So, as proposed by Goldman and Jaluria(198

we choose to determine the jet penetration at the location where the local centreline differe temperature DT, is less than 1% of the exit temperature difference DTO. Furthermore, we hav distinguish the maximum rise of the vertical 'et and the

J

horizontal jet separation from the ceiling. For the first one, an expression has been determine using the general scaling laws of the turbulent buoyant jets proposed by Chen and Rodi (1 9 In this way, we define.

$$Z1 = (z/ho)\ Aro^{213} \quad (4)$$
$$U1 = (Um/U0)\ Aro^{-'13} \quad (5)$$
$$T1 = (DT,/DTO)\ Aro^{-1/3} \quad (6)$$

Figures 5 and 6 show the decay of the centreline velocity and temperature thus obtained. From Figures 5 and 6, we can define the maximum rise of the vertical jet (8p) as.

6 /h, = 0.95 Ar,, -2/3 (7) p

The relation (7) is deduced from the non-dimensional axial distance Z1 equal to 0.95 for which experimental values of the non-dimensionai velocity and temperature difference are zero. L notice that the velocity law given by relation (1) is zero for Z1 equal to 0.90 and then slightly lo than the experimental value. This is due to confinement effect in the short end region (0.9 Z1<0.95) which is not taken into account in the velocity law.
The equation (7) gives lower 8P values than those proposed by Grimitlyn and Pozin (1 9 because of the A value as discussed earlier.

12 ArO=0.00050

Z1 -1 12

Aro=0.00065

10 **U 1 2.12** **Aro=0.001 0**

Aro=0.00104

X **Aro=0.001 1**

8 Z1 -312 113 Aro=0.001 21

U I 9.53 11.13 X

+ Aro=0.00160

6 Aro=0.001 66

ArO=0.001 67

0 Aro=0.001 91

4 **G** ArO=0.00238

Aro=0.00242

Aro=0.00269

2 Aro=0.00353

Aro=0.00428
0 Aro=0.00502
Aro=0.00566

0.0 0.1 **0.2 0.3 0.4 0.5 0.6 0.7 0.8** **0.9 1.0**

Z1

Figure 5. Decay of the centreline velocity of the vertical jet.

we choose to determine the jet penetration at the location where the local centre
difference temperature DT_m is less than 1% of the exit temperature difference I
Furthermore, we have to distinguish the maximum rise of the vertical jet and
horizontal jet separation from the ceiling. For the first one, an expression has b
determined by using the general scaling laws of the turbulent buoyant jets propc
by Chen and Rodi (1980). In this way, we define:

$$Z1 = (z/h_0)\ Ar_0^{2/3} \quad (4$$
$$U1 = (U_m/U_0)\ Ar_0^{-1/3} \quad (5$$
$$T1 = (DT_m/DT_0)\ Ar_0^{-1/3} \quad (6$$

Figures 5 and 6 show the decay of the centreline velocity and temperature t
obtained.
From Figures 5 and 6, we can define the maximum rise of the vertical jet (δ_p) as:

$$\delta_p/h_0 = 0.95\ Ar_0^{-2/3} \quad (7$$

The relation (7) is deduced from the non-dimensional axial distance Z1 equal to C
for which the experimental values of the non-dimensional velocity and temperat
difference are zero. Let's notice that the velocity law given by relation (1) is zero
Z1 equal to 0.90 and then slightly lower than the experimental value. This is du
confinement effect in the short end region (0.90 < Z1<0.95) which is not taken
account in the velocity law.
The equation (7) gives lower δ_p values than those proposed by Grimitlyn and Pc
(1993) because of the A value as discussed earlier.

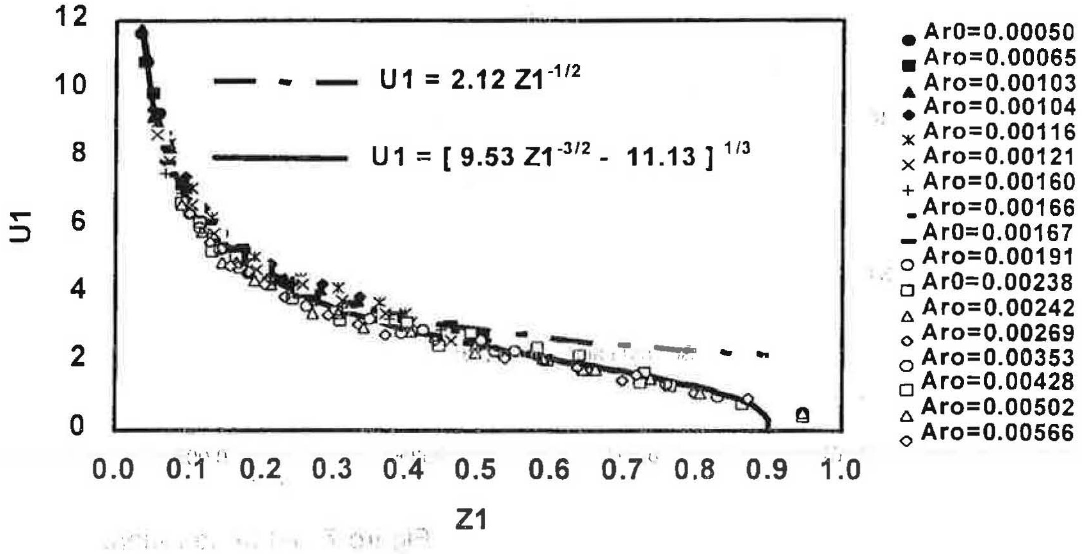

Figure 5. Decay of the centreline velocity of the vertical jet.

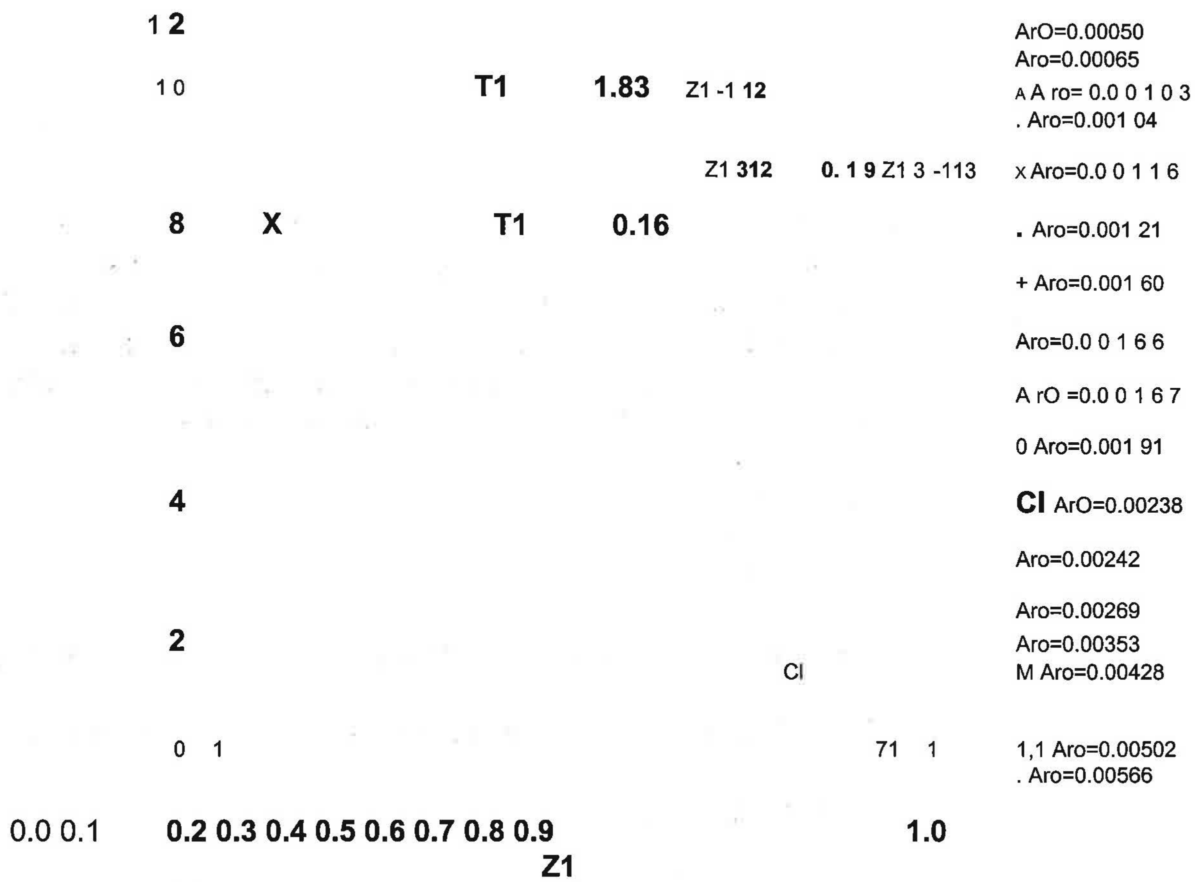

Figure 6. Decay of the centreline temperature of the vertical jet.

Figure 7 shows the jet penetration values for tests when the vertical jet does not reach the ceiling . We notice that the experimental values of the jet penetration along the ceiling are close to relation (7). addition, the empirical law proposed by Goldman and Jaluria (1986) for a warm wall jet diffused down is close to ours.

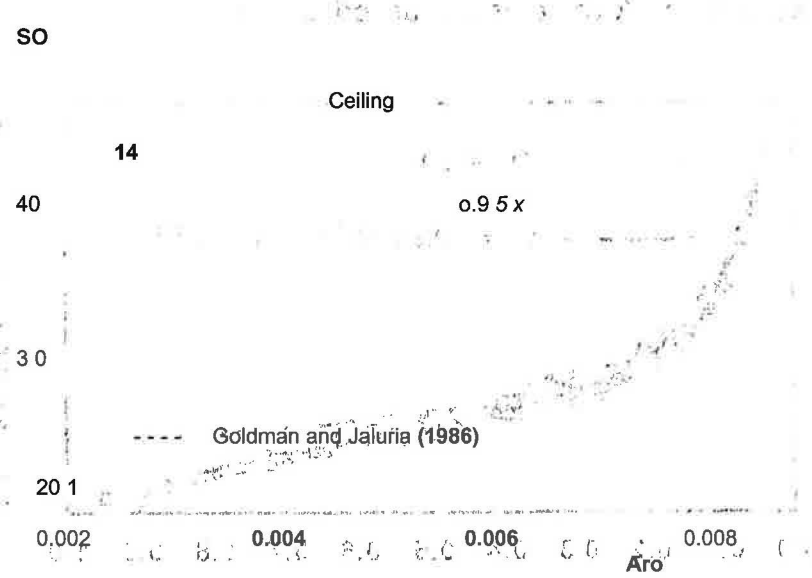

Figure 7. Jet penetration.

4.1.2. Horizontal jet analysis

The wail jet change from a vertical trajectory to a horizontal one at the wall/ceiling corner results in a change of the velocity and temperature decay characteris Measurements of the centreline velocity and temperature profiles taken at different stations downstrea the wall/ceiling corner, are expressed in

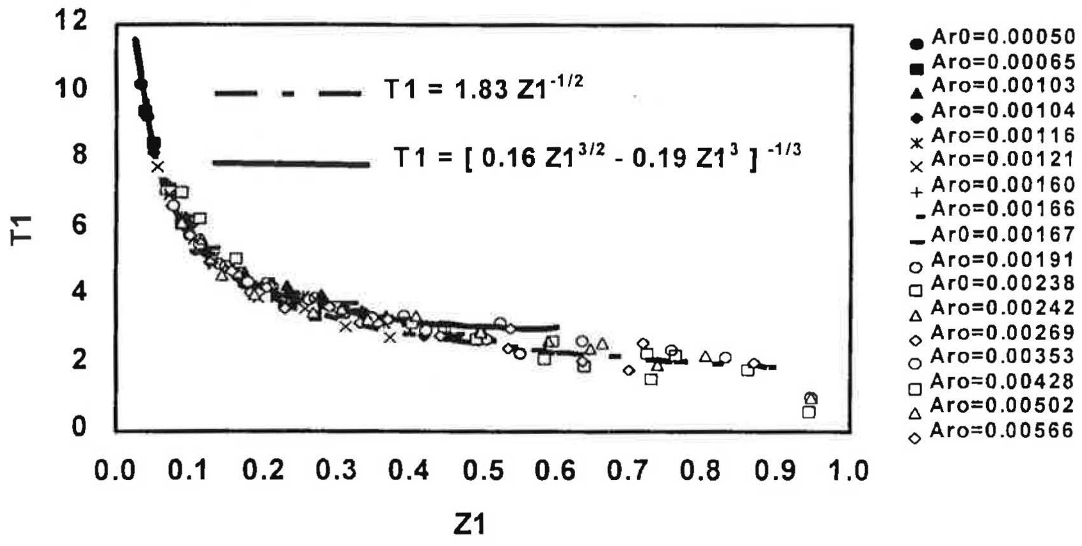

Figure 6. Decay of the centreline temperature of the vertical jet.

Figure 7 shows the jet penetration values for tests when the vertical jet does reach the ceiling . We can notice that the experimental values of the jet penetra along the ceiling are close to relation (7). In addition, the empirical law proposed Goldman and Jaluria (1986) for a warm wall jet diffused downward is close to ours

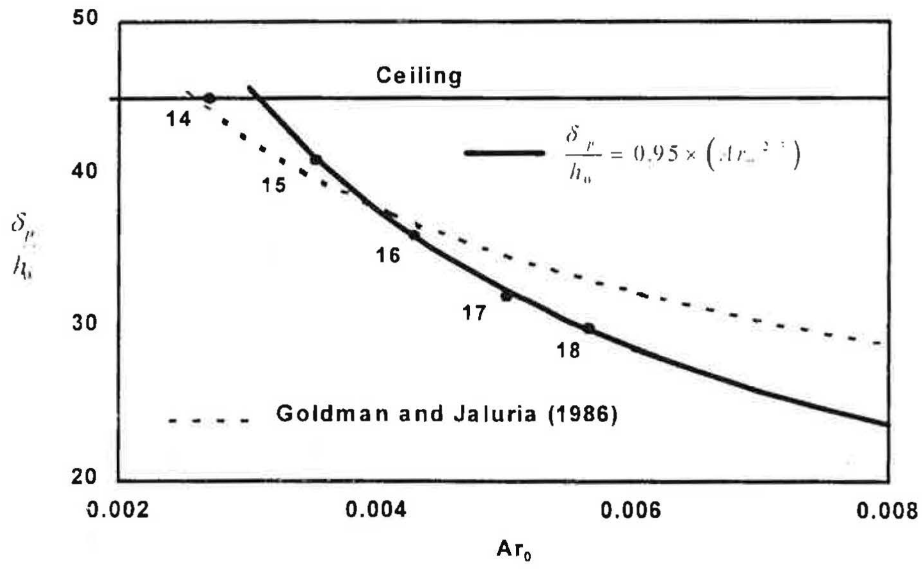

Figure 7. Jet penetration.

4.1.2. Horizontal jet analysis

The wall jet change from a vertical trajectory to a horizontal o at the wall/ceiling corner results in a change of the velocity and temperature dec characteristics. Measurements of the centreline velocity and temperature profi taken at different stations downstream of the wall/ceiling corner, are expressed

terms of the centreline velocity and temperature decay. The x axis is taken along the centre of the jet with an origin at the wall/ceffing corner.
The velocity decay in the isothermal horizontal jet (test 1) is found to be related to the grille a SO and characterized by the presence of three distinct regions in terms of the axis velocity de (Figure 8) indicating a three-dimensional evolution of the jet [Sforza 1970, Sforza 1977, 1976]. Our results are qualitatively very similar to those of the authors and one can disting respectively in the x direction:

a region of flow establishment or potential core..

$UM/U0h = 1$ $\qquad 0 < (x+xo)/ @SO \ 2 \qquad (8)$

a two-dimensional flow region..

$UM/U0h = 1.5 [(x/@S0) -5]-0 5$ $\qquad 2 < (x+xO)/ @SO \ 1 0 \qquad (9)$

an axisymmetric region..

$UM/U0h = 5.6 [(xNS0) -5]\_ 1,08$ $\qquad (x+X0)/ @SO >- 1 0 \qquad (10)$

The virtual origin value xO= -5@Sc) obtained with the isothermal jet is the same that the v proposed by Jackman (1971).

1.0

U 1 UO, = 1.5 [(X+X, Ys 00.5 1-0.5

U 1 U,, = 5.6 [(X+X,)/S01.1 1-108

0.5

xo 5 S,

0.1 1

0.1 1.0 10.0 100.0

(X+XO) 1 S.O.5

Figure 8.. Decay of the centreline velocity of the isothermal horizontal jet.

For the non-isothermai horizontal jet, the velocity and temperature decay are found to be rel to the "horizontal` Archimedes number defined at the wall/ceiling corner
b y..

$ArOh = gPDT0h @SO / U0h \ 2$

terms of the centreline velocity and temperature decay. The x axis is taken along centreline of the jet with an origin at the wall/ceiling corner.
The velocity decay in the isothermal horizontal jet (test 1) is found to be related to grille area S_0 and characterized by the presence of three distinct regions in term the axis velocity decay (Figure 8) indicating a three-dimensional evolution of the [Sforza 1970, Sforza 1977, Sfeir 1976]. Our results are qualitatively very simila those of the authors and one can distinguish respectively in the x direction:

a region of flow establishment or potential core:

$$U_m/U_{0h} = 1 \qquad 0 \leq (x+x_0)/\sqrt{S_0} \leq 2 \qquad (8)$$

a two-dimensional flow region:

$$U_m/U_{0h} = 1.5 \,[\,(x/\sqrt{S_0}) -5\,]^{-0.5} \qquad 2 \leq (x+x_0)/\sqrt{S_0} \leq 10 \qquad (9)$$

an axisymmetric region:

$$U_m/U_{0h} = 5.6 \,[\,(x/\sqrt{S_0}) -5\,]^{-1.08} \qquad (x+x_0)/\sqrt{S_0} \geq 10 \qquad (10)$$

The virtual origin value $x_0= -5\sqrt{S_0}$ obtained with the isothermal jet is the same that value proposed by Jackman (1971).

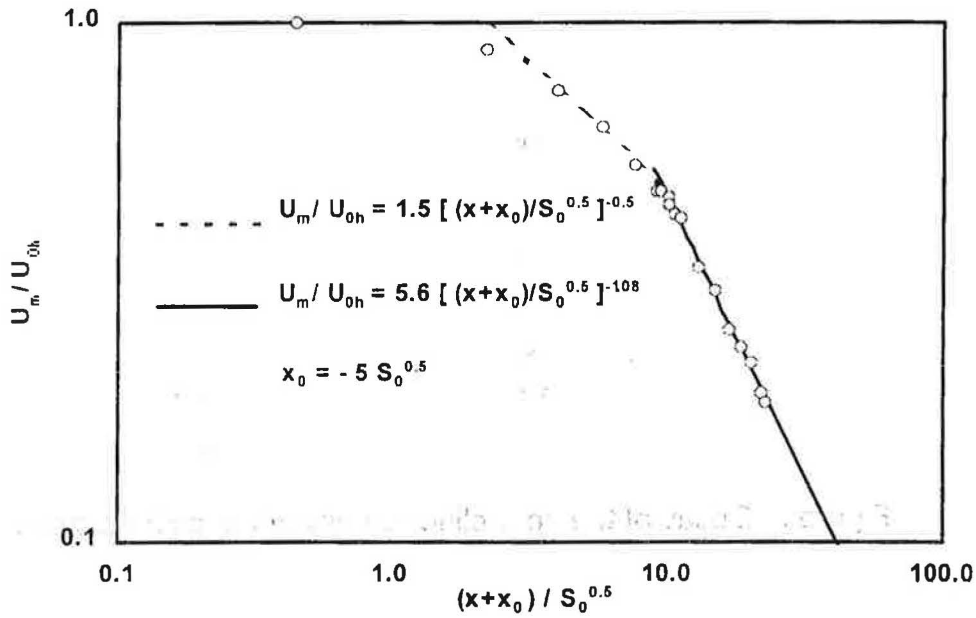

Figure 8: Decay of the centreline velocity of the isothermal horizontal jet.

For the non-isothermal horizontal jet, the velocity and temperature decay are fou to be related to the "horizontal" Archimedes number defined at the wall/ceiling corr by:

$$Ar_{0h} = g\beta DT_{0h} \sqrt{S_0} / U_{0h}^2 \qquad (11)$$

So, in order to study the Archimedes number effect on the centreline velocity temperature in the horizontal jet re-formed along the ceiling, appropriate scaling laws allowe to gather respectively for velocity and temperature every horizontal jets on a same graph. Th scaling laws are defined as.

X 1 = [(x+xo) NS0] ArOh (12)
U 1 h = UM/U0h Aroh- *112* (13)
T1 h = DTM/DT1h ArOh-"2 (14)

Figures 9 and 10 show the decay of the centreline velocity and temperature thus obtained. can distinguish respectively for the velocity and temperature distributions two distinct regi First, the two-dimensional region extends to **X1=0.10.** As in the case of the isothermal jet, non-isothermal jet decays within the two-dimensional region with a decay index n=0.5 an velocity constant Kv=1.5. The velocity distribution in a non-isothermai jet is similar to that in isothermal jet. This confirms the assumption usually done in the literature which is to use isothermal jet law to describe the maximal velocity decay in a horizontal nonisothermal However, as we can see on figures 9 and 10, this assumption is not available anymore in terminal region, where the evolution of the maximal values seems to be closely correlated the Archimedes number. In this region the buoyancy force tends to accelerate the jet diffus particularly for a jet of high Archimedes number.

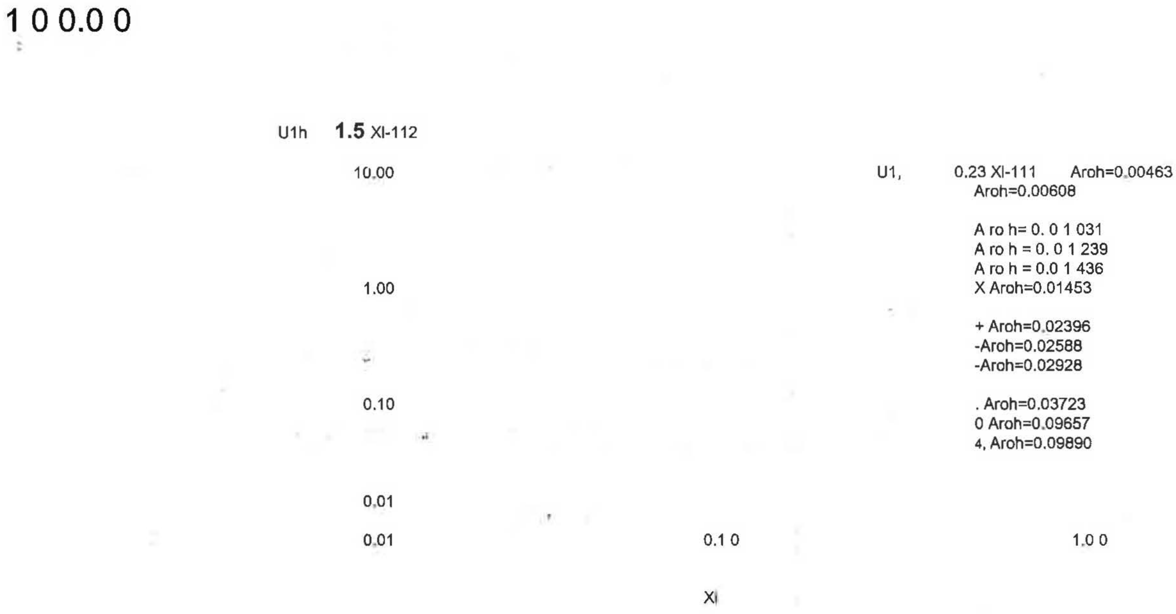

Figure 9. Decay of the centreline velocity of the cold horizontal wall 'et.

J

So, in order to study the Archimedes number effect on the centreline velocity temperature in the horizontal jet re-formed along the ceiling, appropriate scaling l allowed us to gather respectively for velocity and temperature every horizontal on a same graph. These scaling laws are defined as:

$$X1 = [\, (x+x_0)\, /\sqrt{S_0}\,]\, Ar_{0h} \tag{12}$$
$$U1h = U_m/U_{0h}\, Ar_{0h}^{-1/2} \tag{13}$$
$$T1h = DT_m/DT_{0h}\, Ar_{0h}^{-1/2} \tag{14}$$

Figures 9 and 10 show the decay of the centreline velocity and temperature t obtained. One can distinguish respectively for the velocity and temperat distributions two distinct regions. First, the two-dimensional region extends X1=0.10. As in the case of the isothermal jet, the non-isothermal jet decays wi the two-dimensional region with a decay index n=0.5 and a velocity constant K_v=1 The velocity distribution in a non-isothermal jet is similar to that in an isothermal This confirms the assumption usually done in the literature which is to use isothermal jet law to describe the maximal velocity decay in a horizontal n isothermal jet. However, as we can see on figures 9 and 10, this assumption is available anymore in the terminal region, where the evolution of the maximal valı seems to be closely correlated with the Archimedes number. In this region buoyancy force tends to accelerate the jet diffusion, particularly for a jet of h Archimedes number.

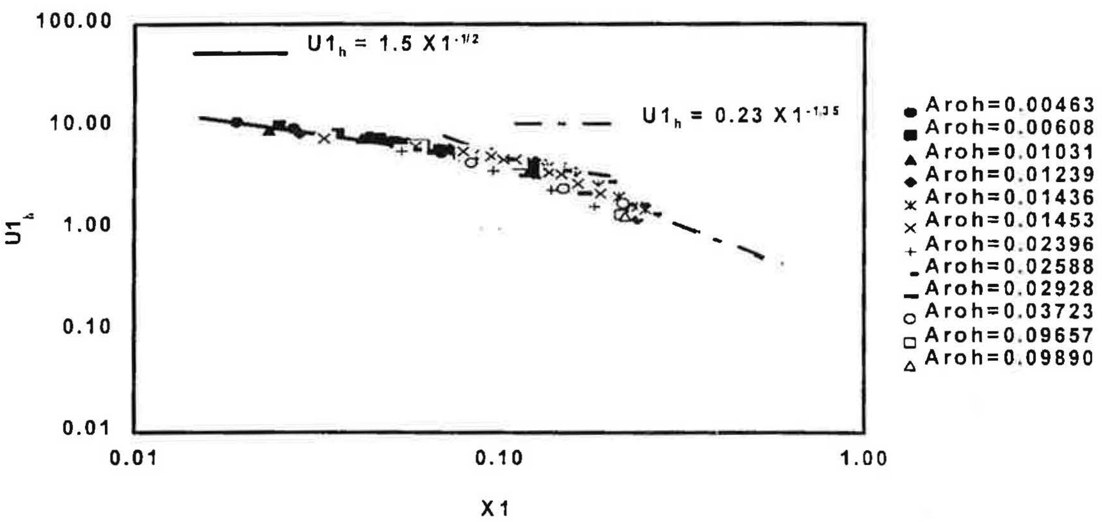

Figure 9. Decay of the centreline velocity of the cold horizontal wall jet.

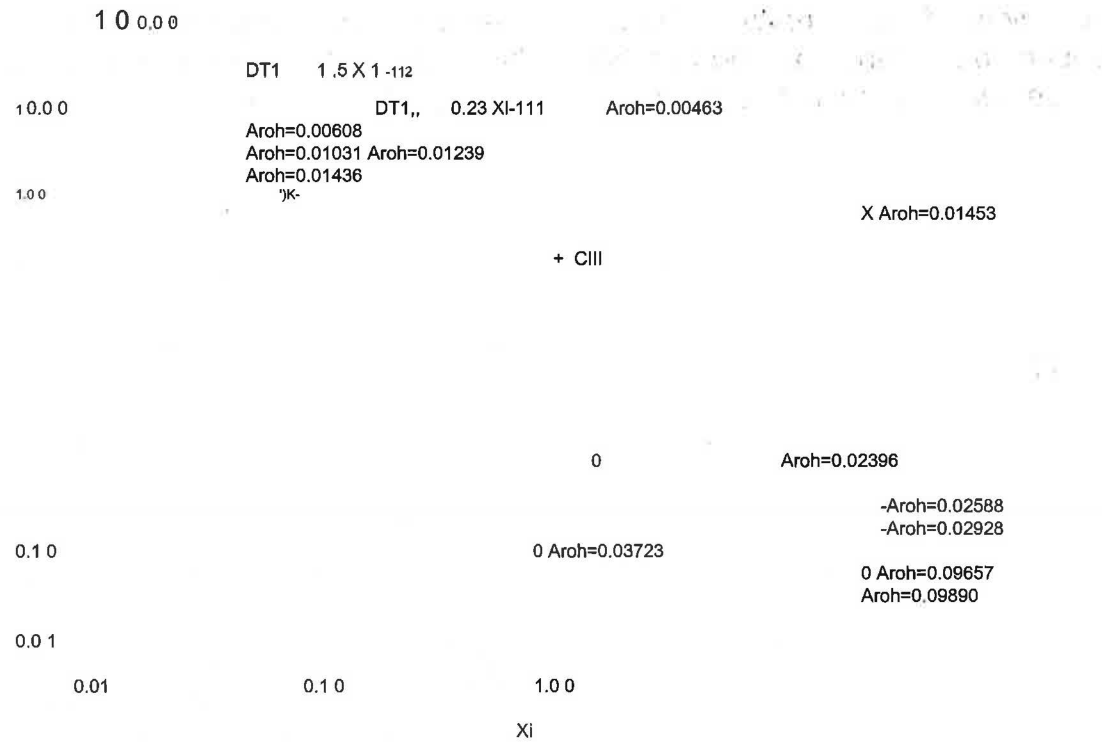

Figure 10. Decay of the centreline temperature of the cold horizontal wall jet.

We measured the distance from the wall/ceiling corner at which the cold jet separates from the ceiling, Xs, due to the downward buoyancy force and we obtained a linear correlation between Xs/@SO and Aro-1 2 (see Figure 1 1). The results can be represented by the following relationship.

(15)

'V S1)

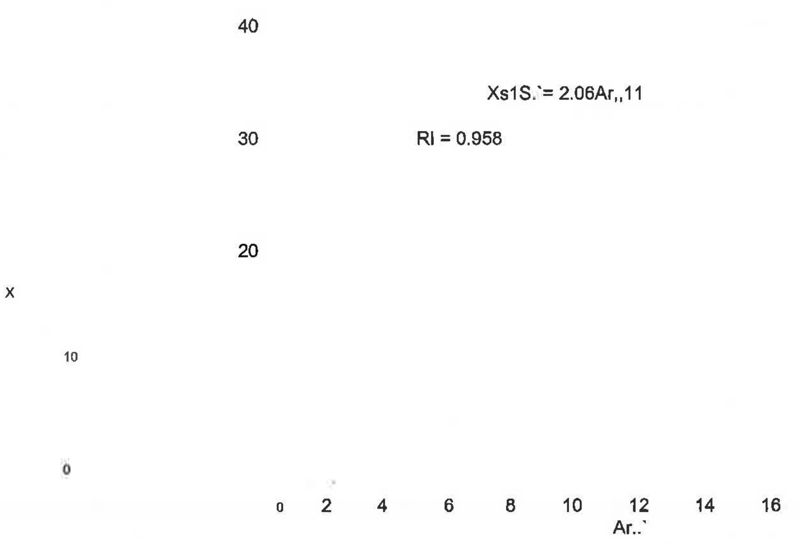

Figure 1 1: Separation distance of the horizontal cold jet

A review of the literature shows that several researchers in this area measured separation distance of a non-isothermal horizontal wall jet. For example Rodahl (1977) presented his results for both linear and axisymmetric jets in the following form..

A's /'(1 1 (16)

- Ca.A

S11

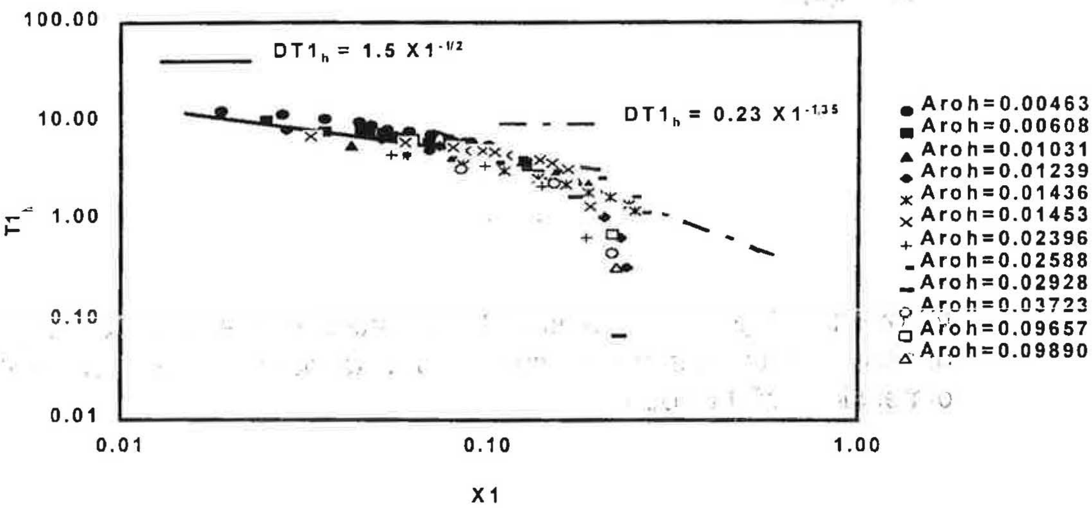

Figure 10. Decay of the centreline temperature of the cold horizontal wall jet.

We measured the distance from the wall/ceiling corner at which the cold separates from the ceiling, Xs, due to the downward buoyancy force and obtained a linear correlation between $Xs/\sqrt{S_0}$ and $Ar_0^{-1.2}$ (see Figure 11). The res can be represented by the following relationship:

$$\frac{Xs}{\sqrt{S_0}} = 2.06.Ar_0^{-1.2} \tag{15}$$

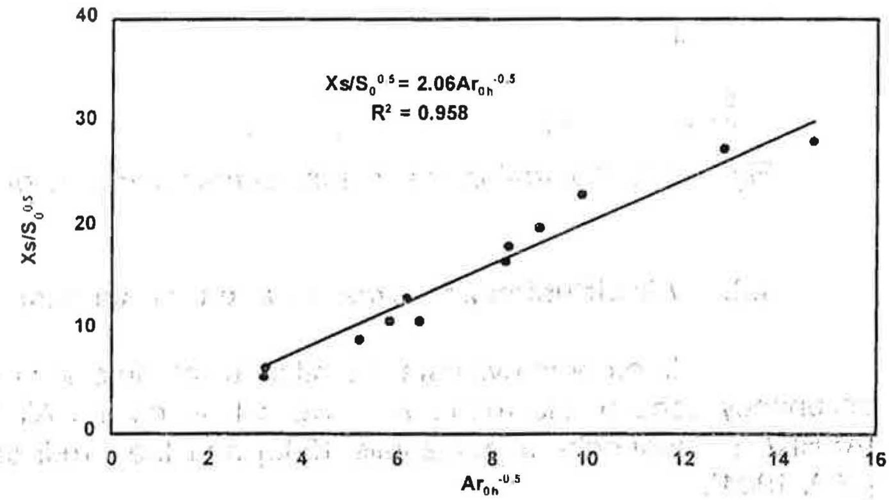

Figure 11: Separation distance of the horizontal cold jet

A review of the literature shows that several researchers in this area measur separation distance of a non-isothermal horizontal wall jet. For example Roda (1977) presented his results for both linear and axisymmetric jets in the followi form:

$$\frac{Xs}{\sqrt{S_0}} = Ca.Ar_0^{-1.2} \tag{16}$$

where the coefficient Ca depends on the jet type and the location of the internal heat loads. an axisymmetric jet and for heat loads supplied from the floor, Rodhai (1 977) reported a valu Ca equal to 2.3. Our experiments show that for the threedimensional jet the separation oc within the axisymmetric region and the experimental data show fairly nice agreement with author's results. In addition some measurements made by different researchers for thr dimensional wall jets

1S -1/2

reported in Figure 12 confirm the variation of the type Xs/ 0-ArOh . Still, the scattering w appears on the Ca value may be due to both the location of the internal heat loads and dimensions of the room.

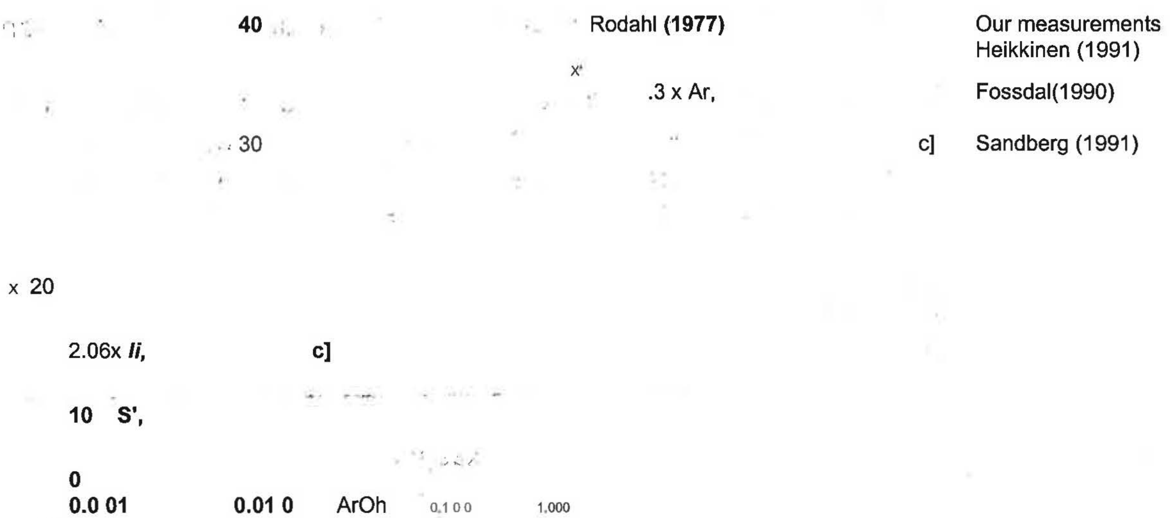

Figure 12. Illustration of some experimental results of separation distance

4.2. Air diffusion performance and thermal comfort

In order to evaluate the influence of the cold air jet and the internal heat loads on occupancy zone of the room, we have calculated the Air Diffusion Performance Index (A [ASHRAE Handbook-Fundamentals 1989] and the Predicted Percentage of Dissatisfied (P [ISO, 1984].

The ADPI is based on the evaluation of the effective draft temperature (EDT) defined in equa (17). The Air Diffusion Performance Index is a percentage which is defined by the numbe points measured in an occupied zone where EDT is within the set limit (>-1.7°C and <`1.1° and the air velocity is less than 0.35m/s over the total number of points measured in the occu zone.

$$EDT = (T_x - T_{a\,mean}) - 8 \cdot (U_x - 0.15) \qquad (17)$$

T_x et U_x: local air temperature and velocity

$T_{a\,mean}$: mean air temperature in the occupied zone

1,1

where the coefficient Ca depends on the jet type and the location of the internal l loads. For an axisymmetric jet and for heat loads supplied from the floor, Ro (1977) reported a value of Ca equal to 2.3. Our experiments show that for the th dimensional jet the separation occurs within the axisymmetric region and experimental data show fairly nice agreement with the author's results. In add some measurements made by different researchers for three-dimensional wall reported in Figure 12 confirm the variation of the type $Xs/\sqrt{S_0} \sim Ar_{0h}^{-1/2}$. Still, scattering which appears on the Ca value may be due to both the location of internal heat loads and the dimensions of the room.

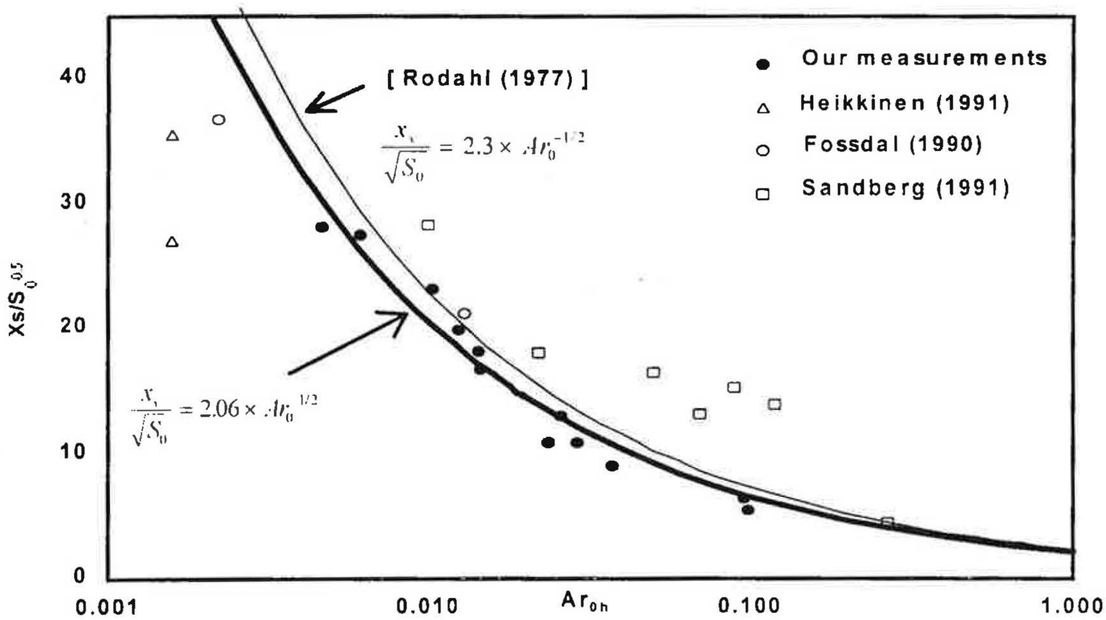

Figure 12: Illustration of some experimental results of separation distance

4.2. Air diffusion performance and thermal comfort

In order to evaluate the influence of the cold air jet and the internal h loads on the occupancy zone of the room, we have calculated the Air Diffus Performance Index (ADPI) [ASHRAE Handbook-Fundamentals 1989] and Predicted Percentage of Dissatisfied (PPD) [ISO, 1984].

The ADPI is based on the evaluation of the effective draft temperature (EDT) defir in equation (17). The Air Diffusion Performance Index is a percentage which defined by the number of points measured in an occupied zone where EDT is wit the set limit (>-1.7°C and <1.1°C) and the air velocity is less than 0.35m/s over t total number of points measured in the occupied zone.

$$EDT=(T_i - T_{a\,mean}) - 8.(U_i - 0.15) \qquad (17)$$

T_i et U_i : local air temperature and velocity

$T_{a\,mean}$: mean air temperature in the occupied zone

Figure 13 shows the experimental values of the ADPI as a function of the 'et Archimedes num Aro.

1.0 **EXP(-146 101 Ar,' + 0.4**
R 2= 0.9074
0.8
0.6
0.4
0.2
0.000 0.002 0.004 0.006

Ar.

Figure 13. ADPI in the occupancy zone of the room.

It can be seen that the ADPI is maximal (100%) for an Archimedes number less than 0.001, then decreases beyond this value as a Gaussian curve with a minimum value of about 4 corresponding to an Archimedes number of 0.006. So, it seems that the ADPI is not related to internal heat loads. This might be attributed to the fact that the ADPI is a measurement of coo mode conditions and only provides the evaluation of velocity and temperature uniformity in room. In fact, the ADPI is based only on air velocity and effective draft temperature combination of local temperature differences from the room average, and is not related to the l of air temperature in the room. In addition, mean radiant temperature which is mostly influen by internal heat loads is not taken into account. Consequently, the use of ADPI to desc thermal comfort may not be adequate. However, it could be considered as a reference valu characterize indoor air flow diffusion.

Fanger (1972), developed a mathematical model to predict the thermal and physiolog response of a human to an environment. The basis of this model is that the internal temperat of the human body remains constant if there is a balance between the heat production by body and the heat loss to the environment. The heat balance equation for a clothed person is.

M±W-E-RES=±K=±R±C (18) where..
M. Metabolism
W. External work
E. Heat exchange by evaporation
RES. Heat exchange by respiration
K Heat conduction through clothing
R. Heat exchange by radiation
C.. Heat exchange by conduction

Figure 13 shows the experimental values of the ADPI as a function of the Archimedes number Ar_0.

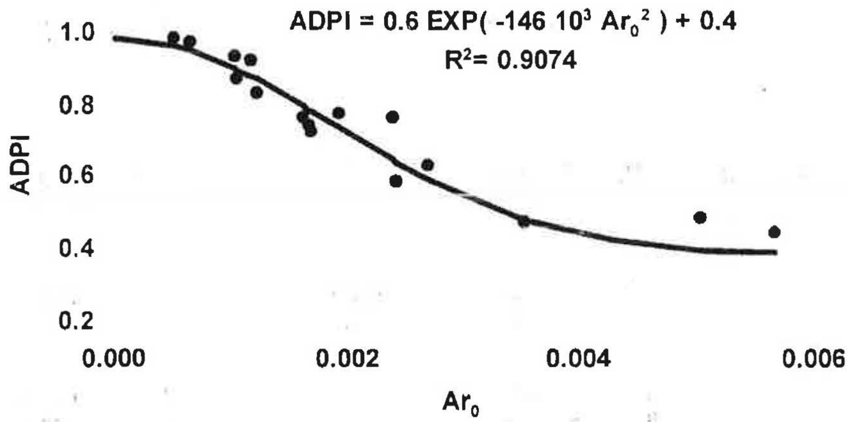

Figure 13. ADPI in the occupancy zone of the room.

It can be seen that the ADPI is maximal (100%) for an Archimedes number less tl 0.001, and then decreases beyond this value as a Gaussian curve with a minim value of about 40% corresponding to an Archimedes number of 0.006. So, it see that the ADPI is not related to the internal heat loads. This might be attributed to fact that the ADPI is a measurement of cooling mode conditions and only provi the evaluation of velocity and temperature uniformity in the room. In fact, the ADP based only on air velocity and effective draft temperature, a combination of lc temperature differences from the room average, and is not related to the level of temperature in the room. In addition, mean radiant temperature which is mo: influenced by internal heat loads is not taken into account. Consequently, the use ADPI to describe thermal comfort may not be adequate. However, it could considered as a reference value to characterize indoor air flow diffusion.

Fanger (1972), developed a mathematical model to predict the thermal a physiological response of a human to an environment. The basis of this model is tl the internal temperature of the human body remains constant if there is a balar between the heat production by the body and the heat loss to the environment. T heat balance equation for a clothed person is:

$$M \pm W - E - RES = \pm K = \pm R \pm C \qquad (18)$$

where:

M: Metabolism
W : External work
E: Heat exchange by evaporation
RES: Heat exchange by respiration
K: Heat conduction through clothing
R: Heat exchange by radiation
C: Heat exchange by conduction

Fanger then developed a procedure, based on the testing of subjects in an environment chamber, to calculate the thermal sensation or Predicted Mean Vote (PMV) given by the following relationship:

PMV = (0.303 e...... m + 0.028) [(M - W)
-3.05 x 10-3 {5.733 - 6.99(M - W) - Pa}
-0.42 {(M - W) -58.15} (1 9)
-1.7 x 10-5 M (5.867 - Pa) 0.0014 M (34 - t,)
-3.96 x 10-8 fd ffid +273) 4 (t, +273)4} - f,, h, (t,, - tJ]

where..

td, 35.7 - 0.028 (M - *W) -0.* 1 55 ICJ [3.96 x 1 0-" fcj {(t,i + 273)4 _ (tr + 273 *)4}* + fc ,1 h,, (t ta

hc	2.28 (tc, - t,)0.25	if	2.28 (t,l - t,)	0,25	> 1 2. 1 \@!v
hc	12.1 @v	if	2.28 (tl - t,)	0,25	< 1 2. 1
f,l	= 1.00 + 0.2 IC1	if	IC1 < 0.5 cio		
fl,	= 1.05 + 0.1 1,1	if	IC1 > 0.5 clo		

2

1C1, Thermal resistance of clothing, clo (1 clo @@.O. 1 55 m K/W
fcl. Ratio of the surface of the area of the clothed body to the surface area of the nude body ta, Room air temperature, °C tr, Mean radiant temperature, "C v. Air velocity, m/s

Pa' Water vapour pressure, Pa

td, Surface temperature of clothing, °C
h.' Convective heat transfer coefficient, W/M2 K

The PMV index gives values over the range -3 to +3 corresponding respectively to cold and hot thermal sensatio Using the PMV value, the Predicted Percentage of Dissatisfied (PPD) can be calculated as:

PPD = 100 - 95 exp[-(0.03353 pMV4 + 0.2176 PMV' A (20)

The lowest value of PPD is 5% dissatisfied corresponding to a PMV of zero and an acceptable maximum of dissatisfied is set to 10% corresponding to a PMV value between -0.5 and +0.5.
The PMV and PPID indices provide an evaluation of comfort for individual points in the occupancy zone. In ord evaluate comfort for the whole room, the Lowest Possible Percentage of Dissatisfied (I-PPD) [Fanger, 19721 is u The LPPD Is calculated using the PMV and PPID of each location in the room. First, the average PMV of the w room is calculated. The mean PMV value will be a negative or a positive value, or zero. If the average PMV is the 1-PPD is simply the mean of

Fanger then developed a procedure, based on the testing of subjects in environmental chamber, to calculate the thermal sensation or Predicted Mean \ (PMV) given by the following relationship:

$$\begin{aligned}PMV = {} & (0.303\, e^{-0.036\, M} + 0.028)\, [(M - W) \\ & -3.05 \times 10^{-3}\, \{5.733 - 6.99(M - W) - P_a\} \\ & -0.42\, \{(M - W) - 58.15\} \\ & -1.7 \times 10^{-5}\, M\, (5.867 - P_a) - 0.0014\, M\, (34 - t_a) \\ & -3.96 \times 10^{-8}\, f_{cl}\, \{(t_{cl} + 273)^4 - (t_r + 273)^4\} - f_{cl}\, h_c\, (t_{cl} - t_a)]\end{aligned} \tag{19}$$

where:

$$\begin{aligned}t_{cl}: = {} & 35.7 - 0.028\, (M - W) - 0.155\, I_{cl}\, [\, 3.96 \times 10^{-8}\, f_{cl} \\ & \{(t_{cl} + 273)^4 - (t_r + 273)^4\} + f_{cl}\, h_{cl}\, (t_{cl} - t_a)]\end{aligned}$$

$$\begin{aligned}h_c &= 2.28\,(t_{cl} - t_a)0.25 && \text{if} \quad 2.28\,(t_{cl} - t_a)^{0.25} > 12.1\sqrt{v} \\ h_c &= 12.1\sqrt{v} && \text{if} \quad 2.28\,(t_{cl} - t_a)^{0.25} < 12.1\sqrt{v}\end{aligned}$$

$$\begin{aligned}f_{cl} &= 1.00 + 0.2\, I_{cl} && \text{if} \quad I_{cl} < 0.5 \text{ clo} \\ f_{cl} &= 1.05 + 0.1\, I_{cl} && \text{if} \quad I_{cl} > 0.5 \text{ clo}\end{aligned}$$

I_{cl}: Thermal resistance of clothing, clo (1 clo $\approx$0.155 m^2 K/W)
f_{cl}: Ratio of the surface of the area of the clothed body to the surface area of the nude body
t_a: Room air temperature, °C
t_r: Mean radiant temperature, °C
v: Air velocity, m/s
P_a: Water vapour pressure, Pa
t_{cl}: Surface temperature of clothing, °C
h_c: Convective heat transfer coefficient, W/m^2K

The PMV index gives values over the range -3 to +3 corresponding respectively cold and hot thermal sensation. Using the PMV value, the Predicted Percentage Dissatisfied (PPD) can be calculated as:

$$PPD = 100 - 95 \exp[-(0.03353\, PMV^4 + 0.2176\, PMV^2)] \tag{20}$$

The lowest value of PPD is 5% dissatisfied corresponding to a PMV of zero and acceptable maximum of dissatisfied is set to 10% corresponding to a PMV val between -0.5 and +0.5.
The PMV and PPD indices provide an evaluation of comfort for individual points the occupancy zone. In order to evaluate comfort for the whole room, the Lowe Possible Percentage of Dissatisfied (LPPD) [Fanger, 1972] is used. The LPPD calculated using the PMV and PPD of each location in the room. First, the avera PMV of the whole room is calculated. The mean PMV value will be a negative or positive value, or zero. If the average PMV is zero, the LPPD is simply the mean

the PPID (P1PID,,,) for the entire space. If the average PIVIV is non-zero then the LIPPID is based on corrected values of the PMV of each location in the room. The corrected values of PIVIV are found by subtracting the average PIVIV from the PIVIV value of each point. With the corrected PIVIV value for each location, the corresponding corrected PIPID value for each point is then found. The LIPPID can then be obtained as the average of the corrected PIPID values for the whole room.
It is convenient to note that the LIPPID index takes a minimum value of 5% in thermally uniform environment and the difference between LPIPID and 5% is a measure of the non-uniformity of the room environment. Fanger (1 972) set a value of 6% as a maximum value for acceptable LIPPID.
The calculation of PMV, PIPID and LIPPID comfort indices were performed for all tests. The maximum value of IPPID (PPDmax) recorded for each test is plotted in Figure 14 against the ratio of internal heat loads to the surface area of the floor.

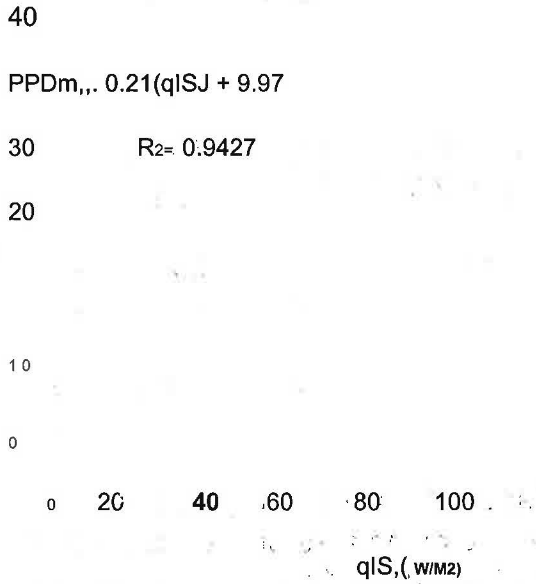

Figure 14. Maximum value of IPPID against internal heat loads

Obviously, there is a fairly good correlation between the maximum value of PPID and internal heat loads. For every tests carried out without internal heat loads the maximum value of PPID is not higher than acceptable maximum of dissatisfied (1 0%). Furthermore, as we can see on Figure 14 the maximum dissatisfied linearly increases as the internal heat loads increases. Consequently, it seems that Archimedes number Aro itself may not be adequate to analyse comfort indices variation. So, in order to study simultaneous effects of supply conditions and internal heat loads, we have defined a corrected Archimedes number Aroc as..

Aroc = gpq/(pCpUO 3 10) (21)

We have plotted respectively on Figures 15, 16 and 17 the percentage of measurement points in the room for which the PPID value is higher than acceptable value of 10%, the average percentage of dissatisfied (PPDm,@,n) and the lowest possible percentage of dissatisfied (LIPPID) against the corrected Archimedes number Aro,

the PPD (PPD_{mean}) for the entire space. If the average PMV is non-zero then LPPD is based on corrected values of the PMV of each location in the room. corrected values of PMV are found by subtracting the average PMV from the F value of each point. With the corrected PMV value for each location, corresponding corrected PPD value for each point is then found. The LPPD can t be obtained as the average of the corrected PPD values for the whole room.
It is convenient to note that the LPPD index takes a minimum value of 5% thermally uniform environment and the difference between LPPD and 5% measure of the non-uniformity of the room environment. Fanger (1972) set a valu 6% as a maximum value for acceptable LPPD.
The calculation of PMV, PPD and LPPD comfort indices were performed for all te The maximum value of PPD (PPD_{max}) recorded for each test is plotted in Figure against the ratio of internal heat loads to the surface area of the floor.

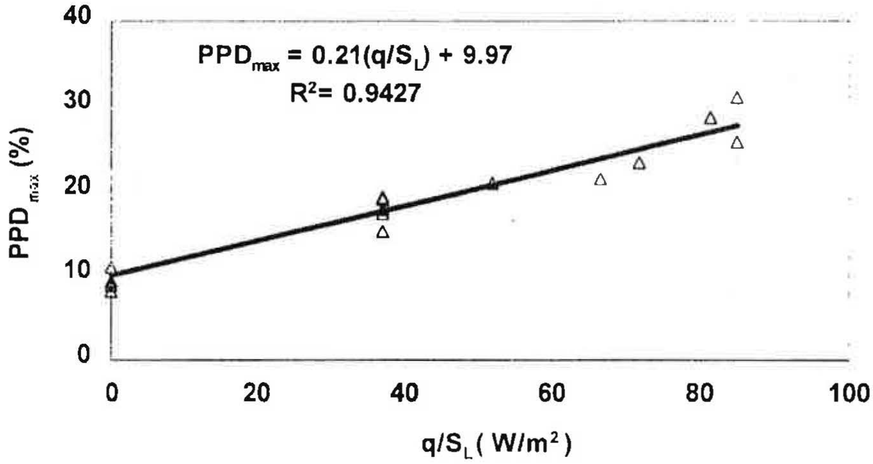

Figure 14: Maximum value of PPD against internal heat loads

Obviously, there is a fairly good correlation between the maximum value of PPD internal heat loads. For every tests carried out without internal heat loads maximum value of PPD is not higher than acceptable maximum of dissatisfied (1(Furthermore, as we can see on Figure 14 the maximum dissatisfied line increases as the internal heat loads increases. Consequently, it seems Archimedes number Ar_0 itself may not be adequate to analyse comfort ind variation. So, in order to study simultaneous effects of supply conditions and inte heat loads, we have defined a corrected Archimedes number Ar_{0c} as:

$$Ar_{0c} = g\beta q/(\rho C p U_0^3 l_0) \qquad (21)$$

We have plotted respectively on Figures 15, 16 and 17 the percentage measurement points in the room for which the PPD value is higher than accept value of 10%, the average percentage of dissatisfied (PPD_{mean}) and the lov possible percentage of dissatisfied (LPPD) against the corrected Archime number Ar_{0c}.

OWPD10 = 9.6 Aro,,0.1
0.8 W= 0.9237

C)

0.6 0
A

0.4

0.2

0

0.000 0.002 0.004 0.006 0.008

ArOC

Figure 15.. Percentage of measurement points above the maximum acceptable PPD

15

10

E

PPDr,,,,n= **47.9** Ar',,:..37+ 5.3

2=
5 R 0.7887

0
0.000 0.002 0.004 0.006 0.008

ArOC

Figure 16.. Average Predicted Percentage of Dissatisfied

7

LPPD = 148.1 ArOC + 5.3
6.5 R2= 0.8754

6
CL
5.5

5

0.000 0.002 0.004 0.006 0.008

Ar.,

Figure 17: Lowest Possible Percentage of Dissatisfied

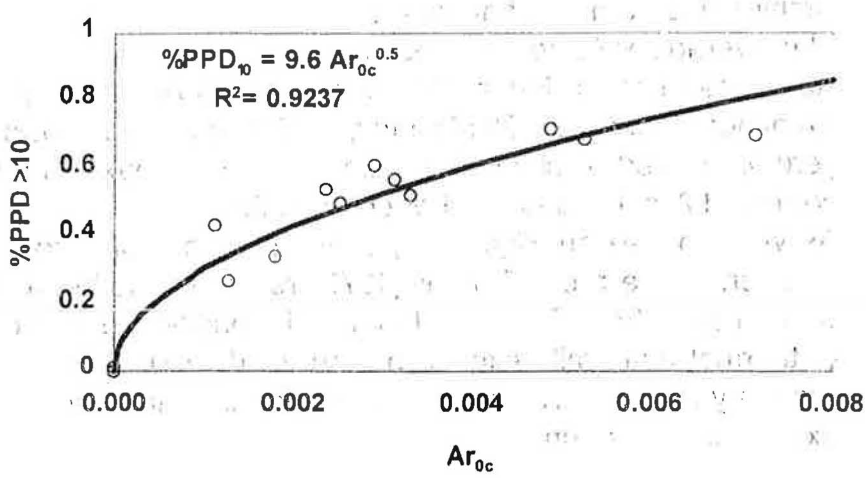

Figure 15: Percentage of measurement points above the maximum acceptable PI

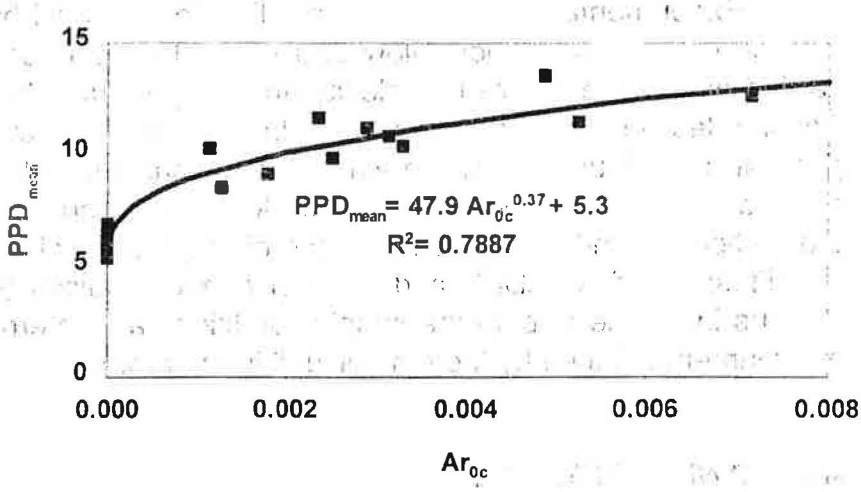

Figure 16: Average Predicted Percentage of Dissatisfied

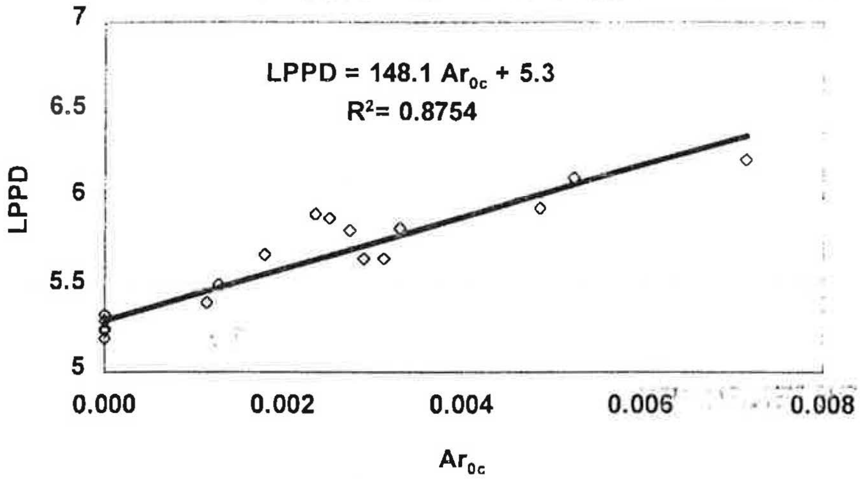

Figure 17: Lowest Possible Percentage of Dissatisfied

It may be seen from Figure 15 that the percentage of measurement points of PPD higher than 10% is zero for all tests which have zero corrected Archimedes number. This agrees with the previous observation concerning the same tests in Figure 14. Furthermore, the percentage value increases versus the corrected Archimedes number as a power correlation and reaches a maximum value of 80% for a corrected Archimedes number of about 0.007.
The average PPD values describe the general thermal comfort obtained in the room. As we can see on Figure 16, these also show a fairly good correlation with corrected Archimedes number. Particularly, PPDmean curve shows a minimum value of 5.3% for zero corrected Archimedes number and a maximum value less than 15% for a corrected Archimedes number equal to 0.007.
As we can see on Figure 17, LPPD is also well correlated to corrected Archimedes number. If we recall Fanger (1972) recommendation of a maximum of 6% for LPPD, we can state from Figure 17 that an air-conditioned environment is satisfactory in terms of thermal uniformity except for corrected Archimedes number higher than 0.005 and precisely for tests 17 and 18 where high internal heat loads were associated to a high exit Archimedes number.

5. CONCLUSION

Experimental studies on the air diffusion induced by a fan-coil unit in a test cell were studied under various flow and internal heat loads conditions. A first analysis carried out on the centreline velocity and temperature showed the influence of the exit Archimedes number on their decay. In this way, we have been able to point out the general behaviour laws of the vertical and horizontal jets. These ones allowed us to deduce a relationship between the exit Archimedes number and both the penetration of the vertical jet and separation distance of the horizontal jet. At last, the analysis of the air diffusion index (ADPI) and thermal comfort indices (PPD and LPPD) shows the obvious influence of both the supply conditions and internal heat loads on the thermal environment induced by the fan-coil unit in the room.

ACKNOWLEDGEMENTS

This study was supported in part by the Environment and Energy Management Agency (ADEME) and Electricity of France (EDF).

REFERENCES

Antonia, R. A., and Chambers A. J. 1980. Errors in simultaneous measurements of temperature and velocity in the outer part of a heated jet. Phys. Fluids, 23(5), May 1980, pp. 871-874.

ASHRAE. 1989. 1989 ASHRAE handbook-fundamentals. Atlanta. American Society of Heating, Refrigerating, and Air-Conditioning Engineers, Inc.

Calvet, P. and Liousse, F. 1971. Mesures locales de temperatures, pressions, vitesses au moyens de capteurs thermor6sistant chauff6s par impulsion. Revue G6,n6rale de Thermique, n' 114.

Chen, C.J. and Rodi W. 1980. Vertical turbulent buoyant jets. A review of experimental data. Pergamon Press, Oxford, United Kingdom.

Fanger P.O., 1972. Thermal Comfort, Analysis and Applications in Environmental Engineering. Toronto, MacGraw-Hill, 1972

Fossdal S_ 1990. Measurement of Testcase E. Internal report for 1EA Annex 20. Norwegian Research Institute, Oslo, 1990.

Goldman, D., and Jaluria, Y. 1986. Effect of opposing buoyancy on the flow in free and wall jets. J. Fluid Mech., Vol. 166, pp. 41-56.

Grimitlyn, M.I. and Pozin, G.M. 1993. Fundamentals of optimizing air distribution in ventilated spaces. ASHRAE Transactions, Vol. 99, Partl, pp. 1128-1138.

Heikkinen J., 1991. Private communication. Technical Research Center of Finland, Espoo,1991.

ISO 7730, 1984. Moderate thermal environments, Determination of the PMV and PPID indices and specifications of the conditions for thermal comfort.

Jackman, P.J. 1971. Air movement in rooms with sill-mounted grilles. A design procedure. BSRiA Lab. Rep. n'71.

Jorgensen, F. E. 1971. Directional sensitivity of wire and fiber film. DISA Information, 1 1, pp. 31-37.

Rajaratnam, N. 1976. Turbulent Jet. Elsevier Scientific Publishing, New York, 1976, 304 p.

Rodahl E., 1977. The point of separation for cold jets flowing along the ceiling. Proceedings of Clima 2000 Conference, Belgrade, Yugoslavia, 1977, pp. 219-228.

Sandberg W 1991. PrixiMP (-.nmmunication . The National Swedish Institute for Building Research, G@vie, 1991.

Sfeir A. A. 1976. The velocity and Temperature Fields of Rectangular Jets. Int. Journal of Heat and 1 vol. 9, Aug. 1976, pp. 1289-1297.

Sforza P. M_ Herbst G., 1970. A Study of Three-Dimensional Incompressible Turbulent Wall Jets. A1AA Journal, 1970, vol. 8, N02, pp. 276-283.

Sforza P. W 1977. Three-Dimentional Free Jets and Wall Jets. Application to Heating and Ventilation. Ant. Seminar of the Int. Center)f Heat and Mass Transfer, 1977, Dubrovnilk Yugoslavia, Aug. 29 Sept. 2, 1970, pp. 283-295

Stannov, T. H. 1995. An accurate, easy to use low-turbulence calibrator for hot-wire anemometers. Dantec Information, 14, pp. 6-1 1.

NOMENCLATURE

Ar Archimedes number

DT air mean difference temperature

CC)

ho exit width of the supply grille (m)

10 exit length of the supply grille (m)

KT decay temperature coefficient

Kv decay velocity coefficient

Q air flow rate (M3 /h)

q internal heat load (W)

SO area of supply grille (M2)

SL floor area (M2)

T air temperature ("C)

U air mean velocity in x or z direction (m/S)

x horizontal distance from the walllceiling corner (m)

xO virtual origin of horizontal jet

z' distance from grille measured vertically up the ceiling and then horizontally across the room from the walllceiling corner (m)

zo virtual origin of vertical jet (m)

3p jet penetration (m)

Subscripts

m centreline value

0 inlet value

Oh wall/ceiling corner value

Xs separation distance (m)

z vertical distance from supply grille (m)